Thoracic aortic geometry correlates with endograft bird-beaking severity

Thoracic aortic geometry correlates with endograft bird-beaking severity

Maxfield M. Frohlich, MS,[a] Ga-Young Suh, PhD,[b] Johan Bondesson, MS,[c] Matthew Leineweber, PhD,[a] Jason T. Lee, MD,[d] Michael D. Dake, MD,[e] *and* Christopher P. Cheng, PhD,[d] *San Jose, Long Beach, and Stanford, Calif; and Göteborg, Sweden*

ABSTRACT

Objective: Aortic geometry has been shown to influence the development of endograft malapposition (bird-beaking) in thoracic endovascular aortic repair (TEVAR), but the extent of this relationship lacks clarity. The aim of this study was to develop a reproducible method of measuring bird-beak severity and to investigate preoperative geometry associated with bird-beaking.

Methods: The study retrospectively analyzed 20 patients with thoracic aortic aneurysms or type B dissections treated with TEVAR. Computed tomography scans were used to construct three-dimensional geometric models of the preoperative and postoperative aorta and endograft. Postoperative bird-beaking was quantified with length, height, and angle; categorized into a bird-beak group (BBG; n = 10) and no bird-beak group (NBBG; n = 10) using bird-beak height ≥5 mm as a threshold; and correlated to preoperative metrics including aortic cross-sectional area, inner curvature, diameter, and inner curvature × diameter as well as graft diameter and oversizing at the proximal landing zone.

Results: Aortic area (1002 ± 118 mm^2 vs 834 ± 248 mm^2), inner curvature (0.040 ± 0.014 mm^{-1} vs 0.031 ± 0.012 mm^{-1}), and diameter (35.7 ± 2.1 mm vs 32.2 ± 4.9 mm) were not significantly different between BBG and NBBG; however, inner curvature × diameter was significantly higher in BBG (1.4 ± 0.5 vs 1.0 ± 0.3; $P = .030$). Inner curvature and curvature × diameter were significantly correlated with bird-beak height ($R = 0.462$, $P = .041$; $R = 0.592$, $P = .006$) and bird-beak angle ($R = 0.680$, $P < .001$; $R = 0.712$, $P < .001$).

Conclusions: TEVAR bird-beak severity can be quantified and predicted with geometric modeling techniques, and the combination of high preoperative aortic inner curvature and diameter increases the risk for development of TEVAR bird-beaking. (J Vasc Surg 2020;72:1196-205.)

Keywords: Thoracic endovascular aortic repair; Endograft; Aortic arch; Bird beak configuration; Endoleak

Thoracic endovascular aortic repair (TEVAR) is a minimally invasive catheter-based technique used to treat aneurysms and dissections in the thoracic aorta. Compared with open surgery, TEVAR offers lower rates of perioperative and early morbidity and mortality, and it continues to gain acceptance as a preferred first-line treatment.[1,2] Despite the advantages of TEVAR, complications that do occur can be severe and warrant reintervention, and they can be challenging to predict preoperatively. Such complications include endograft malapposition (ie, bird-beaking), endoleak, device migration, device collapse, and ischemia.[3]

The bird-beak configuration is defined as an incomplete apposition of the proximal end of the endograft to the aortic lumen wall. It is thought to develop as a consequence of insufficient endograft conformability and hostile aortic geometry (notably, high aortic angulation and curvature) and may be mitigated through active control delivery systems (ie, the ability to orient the proximal endograft in situ).[4-9] Bird-beaking occurs frequently in TEVAR (44%) and is correlated with an increased risk of type IA endoleak in severe cases.[3] Evidence also suggests that severe bird-beaking may lead to premature material fatigue and contribute to device collapse and fracture.[10] It is therefore important to characterize bird-beaking in terms of severity to lessen the occurrence and to mitigate the risk of these complications. Furthermore, this knowledge can assist physicians in optimizing implantation strategy, selecting the device, and evaluating procedure risk with the aim of reducing the severity of bird-beaking.[11] The medical device industry also benefits from insights that may improve the next generation of endografts and delivery systems to better suit hostile anatomy.

Consistent and reliable methods for measuring aortic geometry and bird-beak severity have not been

From the Biomedical Engineering Department, San Jose State University, San Jose[a]; the Department of Biomedical Engineering, California State University, Long Beach[b]; the Division of Dynamics, Chalmers University of Technology, Göteborg[c]; and the Division of Vascular Surgery,[d] and Department of Cardiothoracic Surgery,[e] Stanford University, Stanford.

Author conflict of interest: none.

Correspondence: Christopher P. Cheng, PhD, Division of Vascular Surgery, Stanford University, 1731 Holt Ave, Los Altos, CA 94024 (e-mail: cpc@stanford.edu).

The editors and reviewers of this article have no relevant financial relationships to disclose per the JVS policy that requires reviewers to decline review of any manuscript for which they may have a conflict of interest.

0741-5214

https://doi.org/10.1016/j.jvs.2019.11.045

standardized, which relegates physicians to manual measurements that are subject to significant intraoperator and interoperator variability. Here, we present robust methods for quantifying aortic geometry and bird-beak severity to study how native aortic geometry correlates with the extent of endograft malapposition.

ARTICLE HIGHLIGHTS

- **Type of Research:** Single-center, retrospective cohort study
- **Key Findings:** In 20 patients treated with thoracic endovascular aortic repair (TEVAR), thoracic aortic inner curvature and curvature × diameter were significantly correlated with bird-beak height ($R = 0.462$, $P = .041$; $R = 0.592$, $P = .006$) and bird-beak angle ($R = 0.680$, $P < .001$; $R = 0.712$, $P < .001$).
- **Take Home Message:** TEVAR bird-beak severity can be quantified and predicted with geometric modeling techniques, and the combination of high preoperative aortic diameter and inner curvature is associated with the risk for development of TEVAR bird-beaking.

METHODS

Patient population, imaging, and geometric model construction. This study used retrospective patient data from a previous study that characterized preoperational to postoperational aortic changes in patients who underwent TEVAR with C-TAG (W. L. Gore & Associates, Newark, Del).[12] The original recruitment was based at a single institution and included patients with type B thoracic aortic dissection or thoracic aortic aneurysm (July 2012-March 2015). Patients gave written informed consent, with approval by the local Institutional Review Board, for their imaging data to be used for analysis and publication. From the original 23 patients, three patients with open aortic arch repair were excluded to rule out any influence of open surgery. Computed tomography angiography was performed a median of 37 days before TEVAR and a median of 3 days after TEVAR.

Three-dimensional geometric models of the thoracic aorta and endograft were constructed using the custom software SimVascular (Open Source Medical Software Corporation, San Diego, Calif) by an established method of iterative centerline extraction and two-dimensional orthogonal contour segmentation (Fig 1, *A-D*).[13-15] Of note, the aortic surface was of the true lumen (flow lumen not including the vessel wall), and the endograft was segmented following the center of the metallic struts in cross-sectional views. The centroid of the ostium of the left common carotid artery (LCCA) was identified as a fiducial marker.

Aortic and endograft inner curve extraction. The inner curves of the aorta and endograft were extracted from the aortic and endograft geometries to quantify bird-beak severity and pertinent aortic geometric features. First, the aortic inner curve was defined as the shortest surface path from the beginning of the ascending aorta to the end of the descending thoracic aorta. To estimate this path, we found the center of mass of the thoracic aorta, which was consistently located inferior to the aortic arch lumen (Fig 1, *E*). The center of mass was approximated by computing the mean spatial location of the contours from the right coronary artery to the descending aortic contour located at the same axial level as the starting contour. The first inner surface point was identified as the contour point on the very first contour closest to the aortic center of mass. The centroid-inner surface point pair was then used as a starting point for projecting onto subsequent aortic contours until the entire thoracic aorta was traversed (Fig 1, *F*).[16,17] Optimized Fourier smoothing was then applied to the set of inner surface points and interpolated with 0.1-mm increment to form the final aortic inner curve.[18] By use of the aortic inner curve as a reference line, the points on the endograft contours closest to the aortic inner curve were selected to compose a set of endograft inner surface points, which was subsequently smoothed and interpolated to form the final endograft inner curve (Fig 1, *G*).

Bird-beak metrics. We define bird-beak severity in terms of height, length, and angle using a set of four points (Fig 2). We established these points using the most proximal endograft inner curve point (g_0), the proximal landing point (PLP; a_0), and aorta-endograft apposition points (g_1 and a_1). The PLP is the point on the aortic inner curve closest to the most proximal endograft point. To determine the location of apposition, we accounted for a small separation between the aorta and endograft inner curves (due to distance between metallic struts and contrasted true lumen as well as noise from geometric modeling and inner curve smoothing). The apposition location was chosen by traversing the aortic inner curve in 0.1-mm increments until the pair of endograft-aorta points fell below 3 mm apart. Bird-beak length (BBL) was the Euclidean distance between the proximal endograft inner point (g_0) and the graft apposition point (g_1), bird-beak height (BBH) was the Euclidean distance between the proximal endograft inner point and the PLP on the aorta (g_0 to a_0), and bird-beak angle (BBA) was the angle between the bird-beak line segments of aorta (a_0 to a_1) and endograft (g_0 to g_1).

Preoperative measurements using postoperative endograft location. To gauge preoperative risk of bird-beaking, comparisons were performed between the preoperative geometry and the postoperative bird-beak severity. To extract the preoperative aortic geometry from the segment consistent with the postoperative

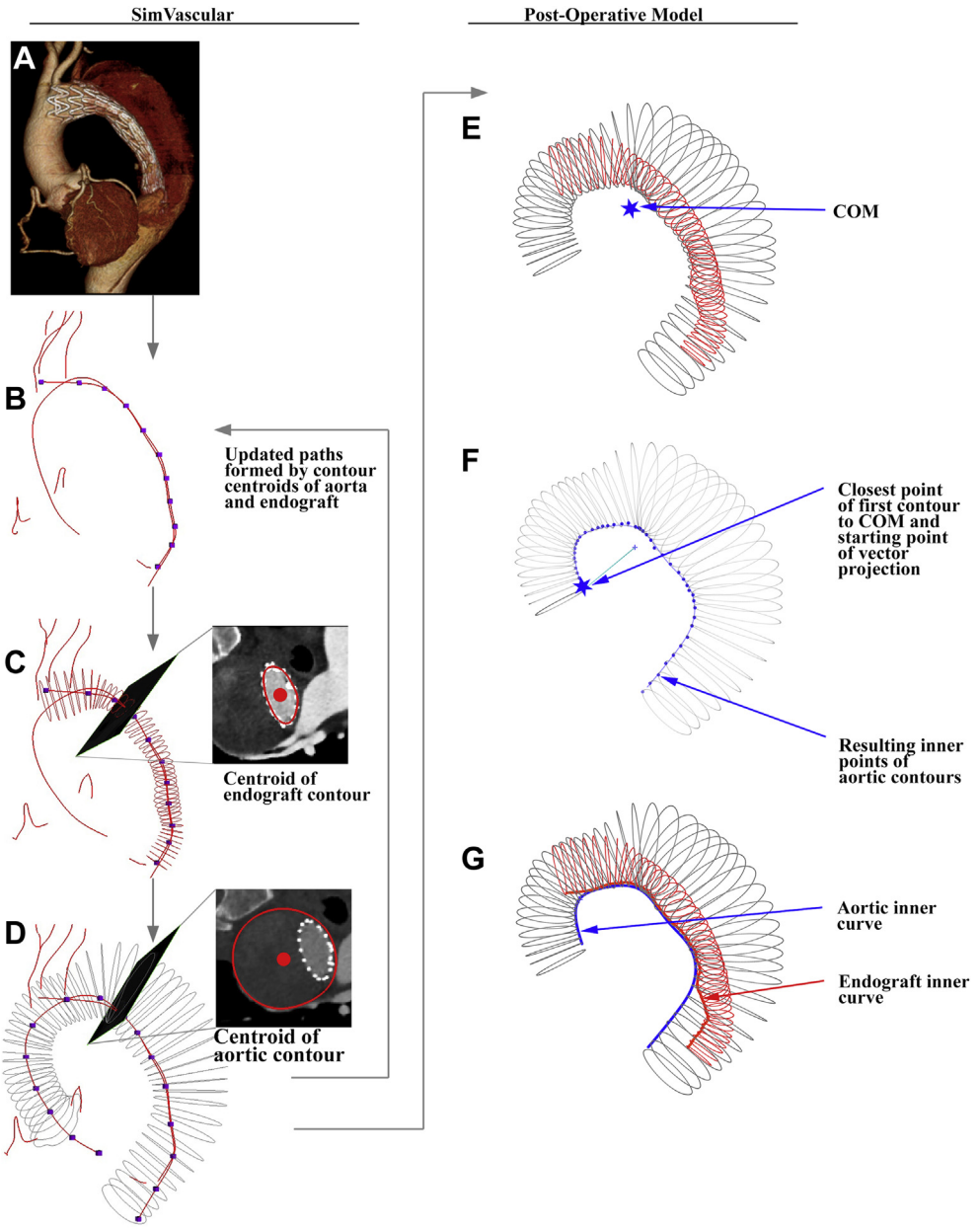

Fig 1. From three-dimensional geometric model creation **(A-D)** to identification of inner curves **(E-G)**. **A,** Computed tomography images (shown rendered) loaded into SimVascular. **B,** Centerline points first selected by hand are splined. **C** and **D,** Aortic and endograft contours are generated orthogonally to their respective centerlines using image segmentation. The contour centroids in **(C)** and **(D)** are used to update the paths in **(B)** to fine-tune the centerline. **E,** Center of mass (*COM*) of the aortic arch calculated from aortic arch centerline. **F,** Closest point on the most proximal aortic contour used to start the vector projection process, from which the inner curve of the aorta was defined. **G,** Aortic inner surface points were Fourier smoothed, and the closest points on the endograft contours were used to form endograft inner curve.

state, preoperative PLP was approximated using the LCCA ostium as a fiducial marker (Fig 3). On the postoperative geometry, the point on the aortic inner curve closest to the LCCA ostium was found, and the arclength distance from that point along the aortic inner curve to the PLP was measured (Fig 3, *A*). Then, that arclength distance was applied to the preoperative inner curve LCCA location to find the corresponding preoperative PLP (Fig 3, *B*).

At the preoperative PLP, longitudinal curvature on the aorta inner curve was measured by using three equally spaced points spanning a 30-mm window size (15 mm between each point) and taking the inverse of the radius of the circumscribed circle fit to those three points.[14]

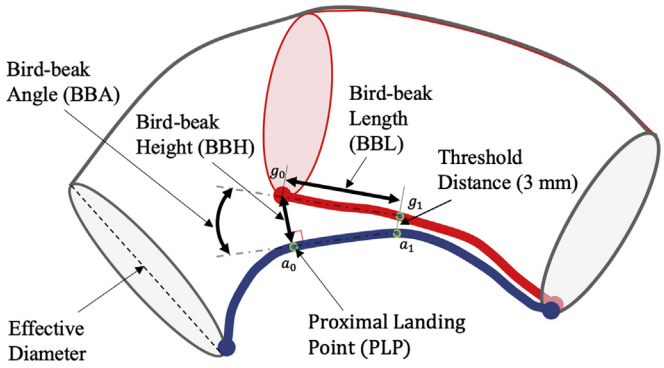

Fig 2. Depiction of outlines of the aortic arch (*gray*) and endograft (*red*) and definition of bird-beak length (*BBL*), bird-beak height (*BBH*), and bird-beak angle (*BBA*). BBH is defined as the shortest distance between the aorta inner curve, referred to as the proximal landing point (*PLP*; a_0), and the proximal point on the endograft inner curve (g_0). The location of aorta-endograft apposition is defined by the most proximal location where the inner curves of the aorta (*thick blue line*) and endograft (*thick red line*) are <3 mm apart (a_1 and g_1).

Effective aortic diameter was calculated along the length of the aorta by using the area of each contour (assuming a circular shape) and linearly interpolating between those contours. The effective diameter at the preoperative PLP could then be extracted. Finally, graft oversizing was defined as the percentage that the proximal graft diameter was larger than the preoperative PLP effective diameter.

Statistical analysis and metric combination. Pearson correlation coefficients (R) and their respective P values were found between preoperative aortic features at the PLP (aortic inner curvature, effective diameter, graft oversizing) and bird-beak severity metrics (BBL, BBH, BBA). In addition, the dimensionless product of inner surface longitudinal curvature × effective diameter was calculated along the aortic inner curve and correlated with bird-beak severity. Thresholds for significant correlations required a P value of <.05 regardless of the strength of R. Strong, moderate, weak, and negligible correlations were defined as follows: strong = $|R| \geq .70$; moderate = $0.70 > |R| \geq .50$; weak = $0.50 > |R| \geq .30$; and negligible = $0.30 > |R|$.[19] Finally, a χ^2 test was performed to determine whether the prevalence of bird-beaking differed by aortic proximal landing zone.

RESULTS

Patients, devices, and geometric measurements. Twenty patients (66 ± 11 years; 16 male) were included in this study for assessment of bird-beak geometry. Patients' characteristics are summarized in Table I, and preoperative aortic metrics (cross-sectional area, inner curvature, effective diameter, curvature × diameter, intended graft oversizing) at the PLP and postoperative bird-beak severity metrics (BBL, BBH, BBA) are reported in Table II. Among the 20 patients in the analysis, 10 exhibited a bird-beak configuration, defined as BBH ≥5 mm. For subgroup analysis, patients with BBH ≥5 mm were assigned to bird-beak group (BBG; n = 10) and others to no-bird-beak group (NBBG; n = 10). The morphologic appearances of the BBG patients depicting their postoperative aortic lumen and endograft models can be found in Fig 4.

Preoperative aortic metrics and postoperative bird-beak severity. Table III shows the resulting calculations for preoperative aortic metrics at the PLP (cross-sectional area, inner surface longitudinal curvature, effective diameter, curvature × diameter, proximal graft diameter, graft oversizing) and postoperative bird-beak severity metrics (BBL, BBH, and BBA) for all patients and the BBG and NBBG populations. Preoperative aortic cross-sectional area, inner curvature, effective diameter, proximal graft diameter, and graft oversizing were not significantly different between the BBG and NBBG populations. However, BBG exhibited significantly greater curvature × diameter compared with NBBG (1.4 ± 0.5 vs 1.0 ± 0.3; $P = .030$). BBG exhibited greater bird-beak severity compared with NBBG in BBL (8.8 ± 3.2 mm vs 1.3 ±1.5 mm; $P < .001$), BBH (7.0 ± 1.7 mm vs 2.5 ± 1.4 mm; $P < .001$), and BBA (28 ± 8 degrees vs 20 ± 10 degrees; $P = .065$). Fig 5 shows color mapped depictions of curvature × diameter along the length of the preoperative aorta for each of the patients in the BBG (*top*) and NBBG (*bottom*) populations. The rate of bird-beaking was not significantly different between aortic zones 2, 3, and 4 for BBG vs NBBG (zone 2: 5 vs 4; zone 3: 3 vs 5; zone 4: 2 vs 1; $P = .624$; Fig 6).

Correlation between preoperative aortic metrics and bird-beak severity. Correlations between preoperative aortic metrics and bird-beak severity metrics are shown in Table IV. Inner curvature was significantly correlated with BBH ($R = 0.462$; $P = .041$) and BBA ($R = 0.680$; $P < .001$), and curvature × diameter was significantly correlated with BBH ($R = 0.593$; $P = .006$) and BBA ($R = 0.713$; $P < .001$). No significant correlations were observed between preoperative metrics and BBL.

DISCUSSION

The algorithm for quantifying preoperative aortic geometry and postoperative bird-beaking severity was successful for all 20 TEVAR patient cases attempted. This

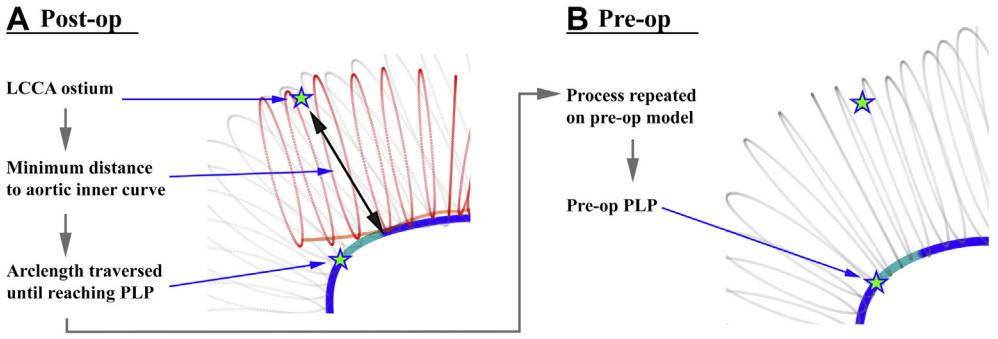

Fig 3. The preoperative proximal landing point (*PLP*) can be estimated using the left common carotid artery (*LCCA*) as a fiducial marker in the postoperative model. **A,** On the postoperative model, the closest point on aortic inner curve to the LCCA ostium is determined, followed by measuring arclength distance to the PLP (shown in *teal*). **B,** The process is repeated on the preoperative model using the LCCA ostium and arclength distance (derived in **A**) to calculate the preoperative PLP.

Table I. Patient and thoracic aortic endograft characteristics

Patient No.	Age, years	Sex	Pathologic process	Device size, diameter × length, mm	Proximal landing zone	Group
1	69	M	D	40 × 200	2	BBG
2	57	M	D	34 × 200	2	NBBG
3	75	M	A	45 × 200, 45 × 150	2	NBBG
4	82	M	D	34 × 200	3	BBG
5	57	M	D	34 × 200, 34 × 150	3	BBG
6	60	F	A	28 × 100	3	NBBG
7	50	F	A	34 × 150, 31 × 100, 31 × 100	4	BBG
8	67	F	A	34 × 150	3	NBBG
9	61	M	D	37 × 200	2	BBG
10	68	M	D	34 × 150, 40 × 150	2	NBBG
11	52	M	D	37 × 200	2	BBG
12	76	M	A	45 × 150, 40 × 150	3	BBG
13	58	M	D	34 × 200, 40 × 150, 45 × 100, 45 × 100	2	BBG
14	89	M	A	37 × 100, 37 × 100	2	NBBG
15	58	F	D	31 × 150	3	NBBG
16	73	M	A	45 × 150, 45 × 150	4	BBG
17	61	M	D	40 × 150	3	NBBG
18	68	M	A	31 × 150, 31 × 150, 31-26 × 100,[a] 31 × 100	3	NBBG
19	66	M	A	34 × 150, 40 × 150	2	BBG
20	82	M	A	40 × 150	4	NBBG

A, Aneurysm; *BBG*, bird-beak group (bird-beak height [BBH] ≥5 mm); *D*, dissection; *NBBG*, no bird-beak group (BBH <5 mm).
Proximal landing zone is the aortic zone where the proximal end of the endograft was deployed.
[a]Tapered graft shown as proximal-distal diameter × length.

study demonstrates that geometric modeling and quantification can be used to standardize the measure of bird-beaking severity and to investigate causative factors preoperatively. We found that high longitudinal inner curvature and large diameter of the aorta, when present at the proximal landing zone, appear to induce a synergistic effect that increases the risk for development of bird-beaking. By color coding curvature × diameter (1/mm*mm), a dimensionless quantity, onto the preoperative aorta, we demonstrate how aortic anatomy may be used to preoperatively map areas with higher risk of malapposition (Fig 5). The evidence supports the notion that

Table II. Preoperative aortic cross-sectional (*CX*) area, inner curvature, effective diameter, curvature × diameter, and intended graft oversizing at the proximal landing point (PLP) and postoperative bird-beak severity described by bird-beak length (*BBL*), bird-beak height (*BBH*), and bird-beak angle (*BBA*)

	Preoperative aortic metrics					Postoperative bird-beak severity metrics			
Patient No.	CX area, mm^2	Inner curvature, mm^{-1}	Effective diameter, mm	Curvature × diameter	Graft oversizing, %	BBL, mm	BBH, mm	BBA, degrees	Group
1	898.2	0.055	33.6	1.8	19	8.3	8.6	43	BBG
2	773.4	0.058	29.7	1.7	15	0.6	3.3	37	NBBG
3	1140.9	0.029	40.1	1.2	12	0.6	1.6	43	NBBG
4	1056.2	0.050	36.2	1.8	−6.1	9.7	6.6	22	BBG
5	816.5	0.038	33.4	1.3	2	6.0	5.7	28	BBG
6	464.5	0.058	24.1	1.4	16	0.3	1.4	26	NBBG
7	1044.4	0.063	37	2.3	−8.2	9.6	9.3	41	BBG
8	599.3	0.029	29.6	0.9	5	0.6	0.8	9	NBBG
9	1003.0	0.035	35.3	1.2	5	12.3	8.9	29	BBG
10	964.4	0.019	34	0.6	0	0.7	1.2	7	NBBG
11	880.5	0.053	33.2	1.8	12	7.2	5.5	21	BBG
12	922.2	0.032	36.3	1.2	10	15.5	8.5	21	BBG
13	1098.9	0.035	38.4	1.3	17	7.8	5.9	23	BBG
14	926.0	0.022	31.2	0.7	19	0.4	3.2	27	NBBG
15	675.0	0.027	32.3	0.9	−4	4.6	4.7	22	NBBG
16	1160.2	0.033	39.8	1.3	0	5.7	5.2	24	BBG
17	1161.7	0.029	37.6	1.1	20	3.4	4.4	26	NBBG
18	588.4	0.032	26.4	0.8	17	0.8	2.5	11	NBBG
19	1143.7	0.032	38.9	1.3	3	5.7	5.4	26	BBG
20	1044.6	0.024	35.8	0.9	12	0.5	1.5	9	NBBG

BBG, Bird-beak group (BBH ≥5 mm); *NBBG*, no bird-beak group (BBH <5 mm).

bird-beaking is a complex, multifactorial phenomenon that is due to a combination of geometric conditions and constraints.

Predicting bird-beaking using the dimensionless metric curvature × diameter makes sense in considering how a tube bends around a curve. Usually, the inner surface shortens while the outer surface lengthens for the tube to maintain a parallel orientation to the curved centerline. Starting from a straight configuration, the endograft implanted into the larger diameter aorta requires more inner curve shortening or outer curve lengthening to maintain a parallel orientation. If the graft material on the outer curve of the endograft is not able to sufficiently lengthen, the endograft would tend to hug the outer curve of the aorta and create malapposition at the inner curve, that is, bird-beaking (Fig 7).

This means that although the aortic geometry is important, device design and its ability to accommodate "hostile" geometry also affect the underlying mechanics of endograft malapposition. Because the graft material used in TEVAR endografts (Dacron or expanded polytetrafluoroethylene) is relatively stiff, the outer surface of the endograft does not stretch with bending, whereas the graft material on the inner curve can wrinkle to accommodate shortening. Simultaneously, the metallic stent rings, which provide outward radial force necessary for wall apposition and stability, are axially rigid and limit the ability to conform to tight inner curves. Endograft designs with lower ring length to diameter ratio, bendable rings, outer curve graft stretchability, or precurved geometries could potentially improve wall apposition in the environment of a large-diameter, curved aorta. Furthermore, delivery systems that allow the surgeon to adjust the orientation of the proximal endograft to the aortic arch may help mitigate or prevent bird-beaking.[9]

Aortic geometry has previously been shown to influence the development of bird-beaking; however, the extent of its influence has not been clearly defined.[4,5,8] Whereas high curvature/angulation at the proximal landing zone has been known to influence bird-beaking, clear relationships between aortic geometry, bird-beak

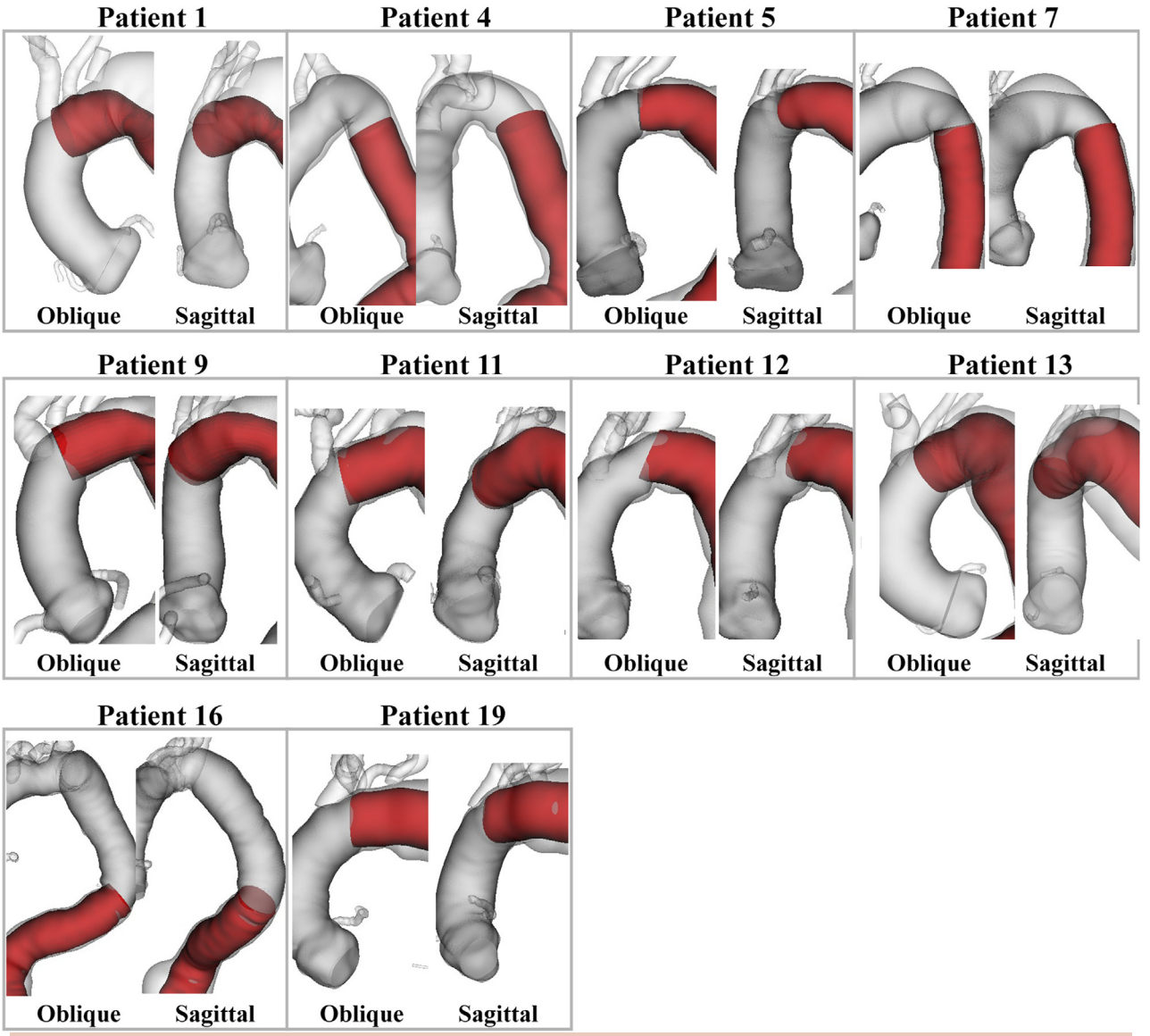

Fig 4. Rendered patient anatomy depicting the aortic lumen (*gray*) with endograft (*red*) in 10 of 20 patients presenting with a bird-beak height (BBH) >5 mm.

Table III. Average preoperative aortic metrics at the proximal landing point (PLP) and postoperative bird-beak severity metrics

	All patients	BBG	NBBG	*P* value
Preoperative metrics				
Cross-sectional area, mm^2	918 ± 208	1002 ± 118	834 ± 248	.068
Inner curvature, mm^{-1}	0.035 ± 0.013	0.040 ± 0.014	0.031 ± 0.012	.133
Effective diameter, mm	34.0 ± 4.1	35.7 ± 2.1	32.2 ± 4.9	.059
Curvature × diameter	1.2 ± 0.5	1.4 ± 0.5	1.0 ± 0.3	**.030**
Proximal graft diameter, mm	37 ± 5	38 ± 4	36 ± 6	.273
Graft oversizing, %	9 ± 8	7 ± 10	10 ± 6	.352
Postoperative bird-beak severity				
BBL, mm	5.0 ± 4.5	8.8 ± 3.2	1.3 ± 1.5	**<.001**
BBH, mm	4.7 ± 2.8	7.0 ± 1.7	2.5 ± 1.4	**<.001**
BBA, degrees	24 ± 10	28 ± 8	20 ± 10	.065

BBA, Bird-beak angle; *BBG*, bird-beak group (BBH ≥5 mm); *BBH*, bird-beak height; *BBL*, bird-beak length; *NBBG*, no bird-beak group (BBH <5 mm). *P* value in bold indicates statistical significance (<.05).

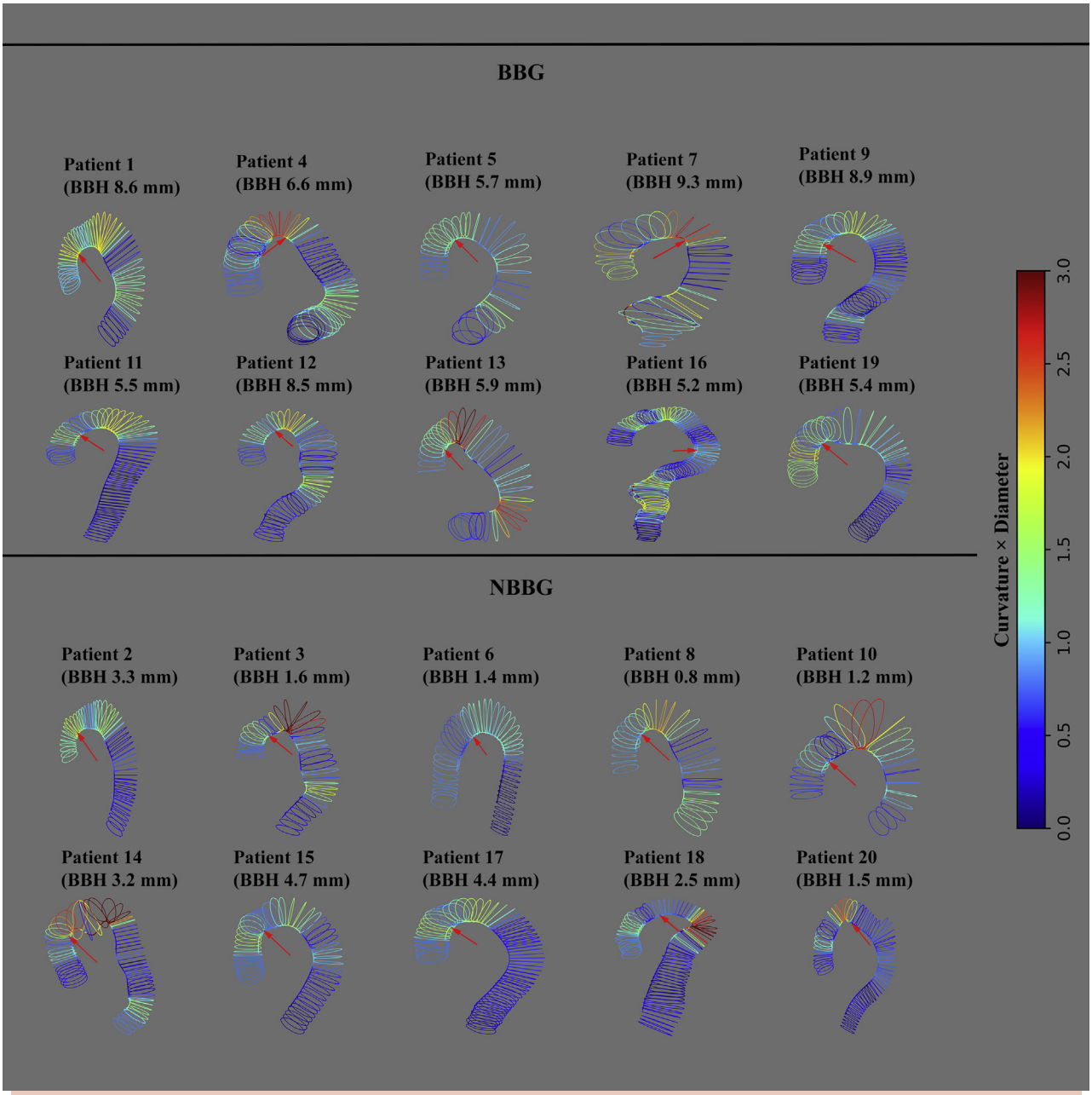

Fig 5. Geometry of preoperative patient aortas depicted by cross-sectional contours for patients with bird-beak height (*BBH*) ≥5 mm (*top*) and BBH <5 mm (*bottom*). The *red arrow* indicates the location of the endograft proximal landing point (PLP) on the preoperative models approximated from the postoperative models (not shown). Color map depicts the product of longitudinal curvature and effective diameter along the inner curve of the aorta; *blue* represents low value of curvature × diameter (small-diameter straight aorta), and *red* represents high value of curvature × diameter (large-diameter curved aorta). *BBG,* Bird-beak group; *NBBG,* no bird-beak group.

severity, and subsequent type IA endoleak have heretofore been lacking.[3-5] This ill-defined relationship may be due to inconsistent, manual methods of measuring bird-beak severity, specifically BBL and BBA, and relating them back to aortic geometry.[3,5,7,8,10] We chose to use BBH as the primary metric for bird-beak severity so that it can be readily quantified with a defined algorithm to improve measurement repeatability. BBL and BBA are less consistent metrics and exhibit higher variability based on the chosen point of apposition between the endograft and aorta, which is in turn highly dependent on the threshold distance between the endograft and

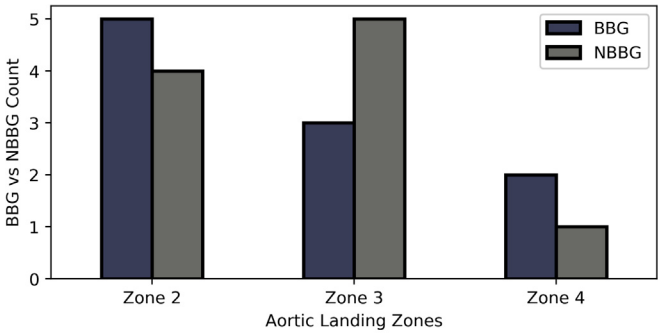

Fig 6. Presence of bird-beaking (bird-beak group [*BBG*], bird-beak height [BBH] ≥5 mm) vs absence of bird-beaking (no bird-beak group [*NBBG*], BBH <5 mm) grouped by proximal aortic landing zone.

Table IV. Correlation of bird-beak severity metrics with preoperative metrics

Bird-beak severity vs preoperative metric	*R* value	*P* value
BBL		
Cross-sectional area, mm^2	0.338	.144
Inner curvature, mm^{-1}	0.291	.213
Effective diameter, mm	0.356	.123
Curvature × diameter	0.421	.0648
Proximal graft diameter, mm	0.235	.318
Graft oversizing, %	−0.152	.522
BBH		
Cross-sectional area, mm^2	0.354	.125
Inner curvature, mm^{-1}	0.462	**.041**
Effective diameter, mm	0.375	.104
Curvature × diameter	0.593	**.006**
Proximal graft diameter, mm	0.223	.337
Graft oversizing, %	−0.198	.403
BBA		
Cross-sectional area, mm^2	0.177	.457
Inner curvature, mm^{-1}	0.680	**<.001**
Effective diameter, mm	0.184	.438
Curvature × diameter	0.713	**<.001**
Proximal graft diameter, mm	0.152	.523
Graft oversizing, %	−0.026	.913

BBA, Bird-beak angle; *BBH*, bird-beak height; *BBL*, bird-beak length. *P* value in bold indicates statistical significance (<.05).

aorta. Conversely, BBH does not rely on establishing a threshold between two lines and can therefore be obtained more consistently and accurately than BBL and BBA. Note, however, that the BBH threshold of 5 mm was chosen to split the patient cohort evenly and that the clinically relevant threshold may in fact be different.

Although there was no significant difference in rates of bird-beaking between zones 2, 3, and 4, there appears to be a trend for more bird beaks to occur in zone 2, as has been shown in the literature.[5] Regardless, we believe that geometric factors, such as curvature × diameter, are more important for determining bird-beaking risk rather than the anatomic definition of the zones themselves.

This study is limited by a small number of patients, all of whom underwent TEVAR with endografts from a single manufacturer and device model. However, we believe that focusing on a single type of endograft helped exclude variability due to endograft variety. Follow-up studies will include larger populations of patients and different endografts (eg, varying conformability) and delivery systems (eg, active control) and will assess interoperator and intraoperator variability, which may point to areas in the algorithm that need to be improved to accommodate additional anatomic and endograft variety. Note that advances in automatic image segmentation (an active area of research in machine learning) may make these methods more feasible in a clinical setting. In addition, future work will include comparison of the proposed methodology with the current "eyeball approach" of vascular surgeons and interventionalists to test whether bird-beak severity can be lessened.

CONCLUSIONS

We developed a consistent, computational method to quantify bird-beak severity in thoracic aorta endografts based on anatomic geometric modeling. Preoperative aortic anatomy, in particular the product of inner curvature and diameter at the proximal landing zone, was significantly predictive of postoperative bird-beak severity, enabling a way to map endograft malapposition risk from preoperative anatomy alone. This predictive model may be helpful for physicians wishing to identify challenging anatomies and specific problem areas for landing zones. In addition, these insights may be used by engineers wishing to design next-generation thoracic endografts.

AUTHOR CONTRIBUTIONS

Conception and design: MF, GS, JL, CC
Analysis and interpretation: MF, GS, JB, ML, JL, MD, CC
Data collection: GS, JL, MD, CC
Writing the article: MF, GS, CC
Critical revision of the article: MF, GS, JB, ML, JL, MD, CC
Final approval of the article: MF, GS, JB, ML, JL, MD, CC
Statistical analysis: MF, ML, CC
Obtained funding: GS, CC
Overall responsibility: CC

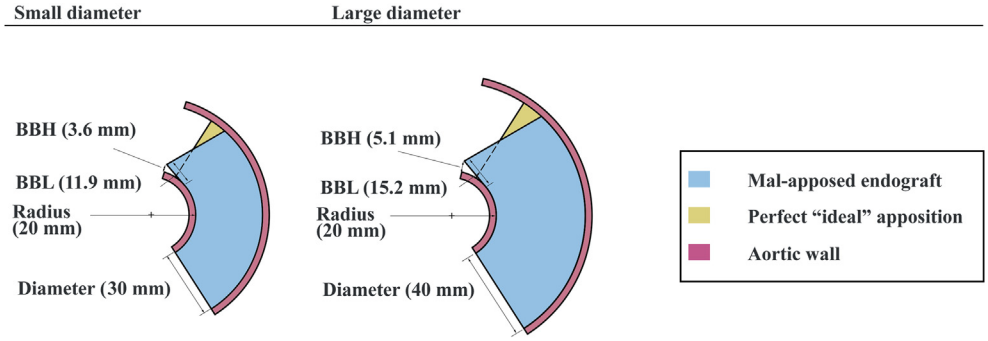

Fig 7. Cross-sectional depiction of aorta (*pink*) and endograft (*blue*) showing a small-diameter aorta (30 mm) and large-diameter aorta (40 mm) with equal inner radius of curvature (20 mm). If the outer curve does not lengthen, as is the case for most endograft material, the larger diameter aorta yields a larger bird-beak height (*BBH*; 5.1 mm vs 3.6 mm) and bird-beak length (*BBL*; 15.2 mm vs 11.9 mm) compared with the smaller diameter.

REFERENCES

1. Dake MD, Miller CD, Semba CP, Mitchell S, Walker PJ, Liddell RP. Transluminal placement of endovascular stent-grafts for the treatment of descending thoracic aortic aneurysms. N Engl J Med 1994;331:1729-34.
2. Fanelli F, Dake MD. Standard of practice for the endovascular treatment of thoracic aortic aneurysms and type B dissections. Cardiovasc Intervent Radiol 2009;32:849-60.
3. Ueda T, Fleischmann D, Dake MD, Rubin GD, Sze DY. Incomplete endograft apposition to the aortic arch: bird-beak configuration increases risk of endoleak formation after thoracic endovascular aortic repair. Radiology 2010;255:645-52.
4. Hsu HL, Chen CK, Chen PL, Chen IM, Hsu CP, Chen CW, et al. The impact of bird-beak configuration on aortic remodeling of distal arch pathology after thoracic endovascular aortic repair with the Zenith Pro-Form TX2 thoracic endograft. J Vasc Surg 2014;59:80-8.
5. Boufi M, Guivier-Curien C, Deplano V, Boiron O, Loundou AD, Dona B, et al. Risk factor analysis of bird beak occurrence after thoracic endovascular aortic repair. Eur J Vasc Endovasc Surg 2015;50:37-43.
6. Pasta S, Scardulla F, Rinaudo A, Raffa GM, D'Ancona G, Pilato M, et al. An in vitro phantom study on the role of the bird-beak configuration in endograft infolding in the aortic arch. J Endovasc Ther 2016;23:172-81.
7. Kudo T, Kuratani T, Shimamura K, Sakamoto T, Kin K, Masada K, et al. Type 1a endoleak following zone 1 and zone 2 thoracic endovascular aortic repair: effect of bird-beak configuration. Eur J Cardiothorac Surg 2017;52:718-24.
8. Kotelis D, Brenke C, Wörz S, Rengier F, Rohr K, Kauczor HU, et al. Aortic morphometry at endograft position as assessed by 3D image analysis affects risk of type I endoleak formation after TEVAR. Langenbecks Arch Surg 2015;400:523-9.
9. Kölbel T, Larena-Avellaneda A, Diener H, Debus ES. The "Pro-Form" modified Zenith TX2 thoracic endograft. Conformability + conformation = conformance: the importance of fitting the graft to the vessel. J Endovasc Ther 2010;17:471-3.
10. Rinaudo A, Raffa GM, Scardulla F, Pilato M, Scardulla C, Pasta S. Biomechanical implications of excessive endograft protrusion into the aortic arch after thoracic endovascular repair. Comput Biol Med 2015;66:235-41.
11. Kölbel T, Resch TA, Dias N, Björses K, Sonesson B, Malina M. Staged proximal deployment of the Zenith TX2 thoracic stent-graft: a novel technique to improve conformance to the aortic arch. J Endovasc Ther 2009;16:598-602.
12. Ullery BW, Suh GY, Hirotsu K, Zhu D, Lee JT, Dake MD, et al. Geometric deformations of the thoracic aorta and supra-aortic arch branch vessels following thoracic endovascular aortic repair. Vasc Endovascular Surg 2018;52:173-80.
13. Wilson N, Wang K, Dutton RW, Taylor C. A software framework for creating patient specific geometric models from medical imaging data for simulation based medical planning of vascular surgery. Lect Notes Comput Sci 2001;2208:449-56.
14. Suh GY, Beygui RE, Fleischmann D, Cheng CP. Aortic arch vessel geometries and deformations in patients with thoracic aortic aneurysms and dissections. J Vasc Interv Radiol 2014;25:1903-11.
15. Cheng CP, Zhu YD, Suh GY. Optimization of three-dimensional modeling for geometric precision and efficiency for healthy and diseased aortas. Comput Methods Biomech Biomed Engin 2018;21:65-74.
16. Lundh T, Suh GY, DiGiacomo P, Cheng C. A Lagrangian cylindrical coordinate system for characterizing dynamic surface geometry of tubular anatomic structures. Med Biol Eng Comput 2018;56:1659-68.
17. Bondesson JH, Suh GY, Lundh T, Lee JT, Dake MD, Cheng C. Automated quantification of diseased thoracic aortic longitudinal centerline and surface curvatures. J Biomech Eng 2019 Oct 1. [Epub ahead of print].
18. Choi G, Cheng CP, Wilson NM, Taylor CA. Methods for quantifying three-dimensional deformation of arteries due to pulsatile and nonpulsatile forces: implications for the design of stents and stent grafts. Ann Biomed Eng 2009;37:14-33.
19. Hinkle D, Wiersma W, Jurs S. Applied statistics for the behavioural sciences. 5th ed. Boston: Houghton Mifflin; 2003.

Submitted Aug 21, 2019; accepted Nov 22, 2019.